HPFRCC-4, 4th international Workshop on High Performance Fiber Reinforced Cement Composites

Ann Arbor, Michigan, USA, June 16-18, 2003

# Structural behavior of hybrid elements with Advanced Cementitious Materials (HPFRCC)

Emmanuel Denarié, Katrin Habel, Eugen Brühwiler
Laboratory of Maintenance and Safety of Structures, Institute of Structures, School of Architecture, Civil and Environmental Engineering, Swiss Federal Institute of Technology, Lausanne (EPFL), Switzerland

Abstract

Advanced Cementitious Materials such as HPFRCC are well adapted for durable repair and strengthening of concrete structures. Experimental and numerical investigations have been conducted to study the behavior of hybrid structural elements consisting of HPFRCC and ordinary concrete. The behavior at service state as well as at ultimate limit state of the beams reinforced with HPFRCC was comparable or better than the behavior of the beams reinforced with ordinary reinforced concrete. The sensitivity of numerical models for hardening materials such as HPFRCC was demonstrated.

## 1. Introduction

The outstanding properties of Advanced Cementitious Materials such as HPFRCC (very high strength and very low permeability) can be used in new or existing structures. In hybrid structures formed of old and new concretes, these materials offer a high potential in view of the protective and load carrying function of the new layer as illustrated in Fig. 1.

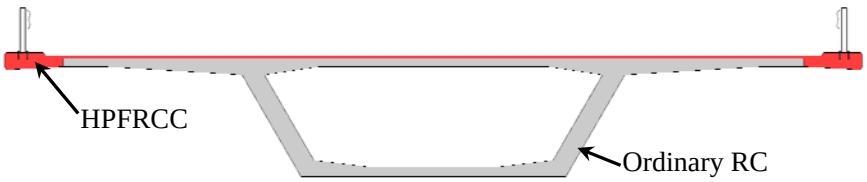


Fig. 1. Conceptual vision of a hybrid bridge deck with a protective layer of HPFRCC.

The tensile behavior and resistance to cracking of HPFRCC, alone or combined with high performance reinforcements, open innovative perspectives in view of the carrying

capacity. In order to fully benefit from all those properties, one has (1) to be able to characterize them experimentally in a reliable and representative way at the material and at the structural level, and (2), to have numerical models able to reproduce the observed behavior and predict the response of structural elements.
With these aims in view, an experimental campaign has been undertaken to determine the tensile behavior of HPFRCC and the structural response of hybrid elements made of ordinary concrete and HPFRCC. The performance of various numerical models to reproduce the structural response of the hybrid beams was studied; discrete and smeared crack approaches were compared and discussed.

## 2. Experimental

### 2.1 Materials

The new layer consisted either of reinforced concrete (RC), one classical type of steel-fiber-reinforced concrete (SFRC) with hooked Dramix fibers or an HPFRCC: Ductal® [1], the old layer was always ordinary concrete (Table 1). The ready premix of the HPFRCC consisted of cement, silica fume, fine sand and quarz powder.

Table 1: Material composition

| | **Old Concrete** | **Reinforced Concrete** | **SFRC** | **HPFRCC** |
|---|---|---|---|---|
| Cement [kg/m$^3$] | 328 | 328 | 319 | ready premix |
| Water/Binder | 0.49 | 0.49 | 0.54 | 0.14 |
| Reinforcement | no | 51 kg/m$^3$<br>2 ∅ 8 | 74 kg/m$^3$<br>30mm/0.5mm<br>hooked | 165 kg/m$^3$<br>13 mm/0.15 mm<br>straight |

### 2.2 Mechanical properties

The compressive strength $f_{c,cyl}$ and Young's modulus $E_{cc}$ of the materials were determined using cylinders (l = 32 cm, ∅ = 16 cm) and the maximal tensile stress $f_{ct}$ was determined on prismatic notched specimens (section: 10*10 cm$^2$) at 28 days (Table 2).

Table 2: Material properties of the materials for the hybrid beams

| | **Old Concrete** | **Concrete** | **SFRC** | **HPFRCC** |
|---|---|---|---|---|
| $f_{ct}$ [N/mm$^2$] | 2.7 | 2.7 | 3.1 | 7.4 |
| $f_{c,cyl}$ [N/mm$^2$] | 31.8 | 31.8 | 35.8 | 170.7 |
| $E_{cc}$ [N/mm$^2$] | 31'000 | 31'000 | 29'100 | 56'500 |

The overall tensile behavior of the HPFRCC in the new layer was determined by means of an instrumented test, on notched plates with a section of 160 x 50 mm$^2$ extracted from the bottom face of the beams, in the non-loaded zones of the remaining two halves of the beams, after the flexural test was completed, The system, Fig. 2., designed and tested until a maximal stress of 30 MPa in the specimen's cross section, is particularly well adapted for cementitious materials with a high tensile strength such as HPFRCC.

The principle of the test is similar to the one used by Helbling and Brühwiler [2], Fig. 2. A metallic base plate (b) is fixed on the testing machine e), with four bolts. Metallic pieces (a) with horizontal grooves on their inner side (the side facing the specimen) are fixed on this plate. The pieces (a, b) are treated with a mould-release agent. The space between the metallic pieces (a) and the specimen (c) is filled with glue (d), assuring a stress transfer by adherence between the specimen (c) and the glue (d), and a stress transfer by interlocking between the glue (d) and the metallic pieces (a). As the specimen is not bonded to the surrounding metallic pieces, its lateral contraction is not restrained, and the risk of fracture in the anchoring zone is reduced to a large extend. As the specimen is built-in in the surrounding metallic pieces, a stiff connection can be obtained, which contributes to the overall stiffness of the test set-up. An additional benefit of this test setup is that the surrounding metallic pieces can easily be reused after a test.

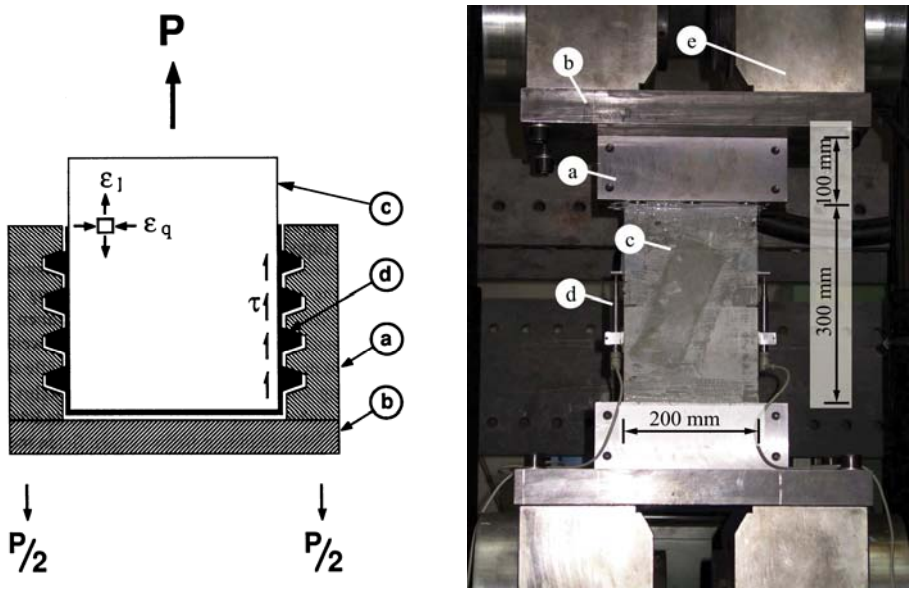


a) b)

Fig. 2. Set-up of the uniaxial tensile test: a) principle, b) complete set-up with a built-in notched specimen.

The tensile tests were carried out on a 1000 kN universal testing machine with a hydraulic actuator, and displacement controlled using a closed-loop. The reference displacement was determined using the mean value of two LVDTs (Fig. 2b, (d)) mounted on the sides of the specimen. More details on this test can be found in [3].

Fig. 3 presents the observed behavior for the two plates extracted from the hybrid beams, after testing. The maximum tensile stress is around 8 $N/m^2$ which is lower than the expected value around 10 $N/mm^2$ usually found in the literature for this material, [1].

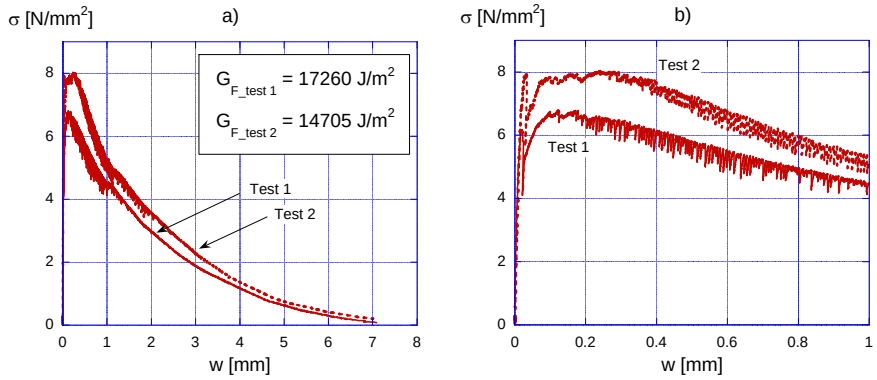


Fig. 3. Tensile tests on notched plates extracted from the new layer in HPFRCC of the hybrid beams, a) general, b) detail.

### 2.3 Structural tests on hybrid beams

Hybrid concrete beams were tested in 3-point-bending, [4]. Two beams of each type of New Layer (NL) were tested. The surface, on which the new layer was cast, was prepared by hydrodemolition. The beams were tested, when the new layer was 28 days old, whereas the old layer was at least 60 days old. The displacements were measured in the middle of the span ($f_2$) and above the supports ($f_1$ and $f_3$), such that the deflection could be calculated with $f_2-(f_1+f_3)/2$. Ω-gages were used vertically at the interface ($w_{10}$, $w_{11}$, $w_{12}$) and horizontally in the middle of the span ($w_{13}$, $w_{14}$, $w_{15}$) to follow the crack mouth opening displacement (CMOD) and monitor possible delaminations following the propagation of through cracks in the new layer. The tests were displacement-controlled by a hydraulic jack in the middle of the span with a speed of 3.6 mm/hour at the beginning until a deflection of 4 mm and 72 mm/hour for the rest of the test.

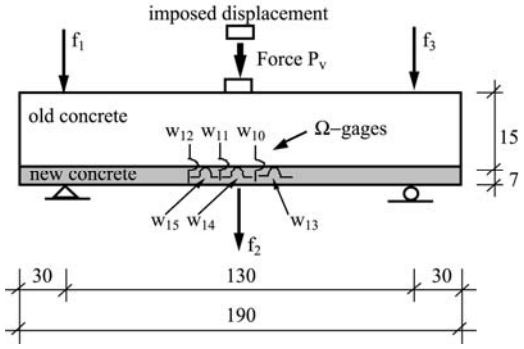


Fig. 4. Three point bending test on hybrid beams (thickness 22 cm).

Fig. 5 presents the force-deflection curves for all the beams tested. The results obtained on beams reinforced with similar materials show a good correspondence. The beams reinforced with RC and the beams reinforced with HPFRCC reached nearly the same peak force, whereas the beams reinforced with SFRC showed much lower peak forces. In

this configuration, the reinforcement with HPFRCC equals the reinforcement with RC in terms of maximum carrying capacity. It is better in terms of pre-peak stiffness and shows a significant descending branch with a residual carrying capacity of 50 % of the maximum at peak force, for the deflection where the yield point of the reinforcement bars is attained in the case of the beams reinforced with RC. As expected, the reinforcement effect provided by the short fibers leads to a gradual descending branch.

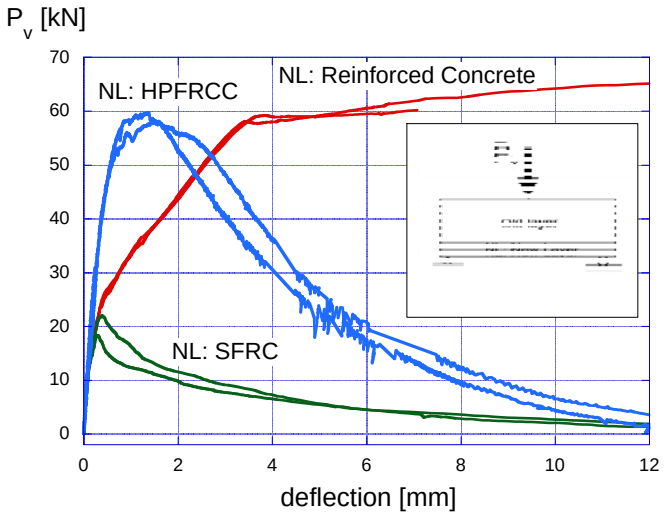


Fig. 5. Experimental tests on the hybrid beams, force-deflection response as a function of the material used for the new layer (NL).

Fig. 6 shows the work as a function of the deflection for all the beams. First of all, one can see that until the point where the yield point of the reinforcement in the new layer of RC is reached, the energy dissipated by the beams reinforced with HPFRCC is larger than that dissipated by the beams reinforced with RC. This effect could be attributed to the multiple pull-out processes of fibers involved in the progressive cracking of the HPFRCC. This frictional mechanism appears more efficient in terms of energy dissipation than the mechanisms involved in the cracking of reinforced concrete, prior to yielding of the reinforcement bars. Yielding of the reinforcement bars in the new layer is revealed by a straight line after point B.

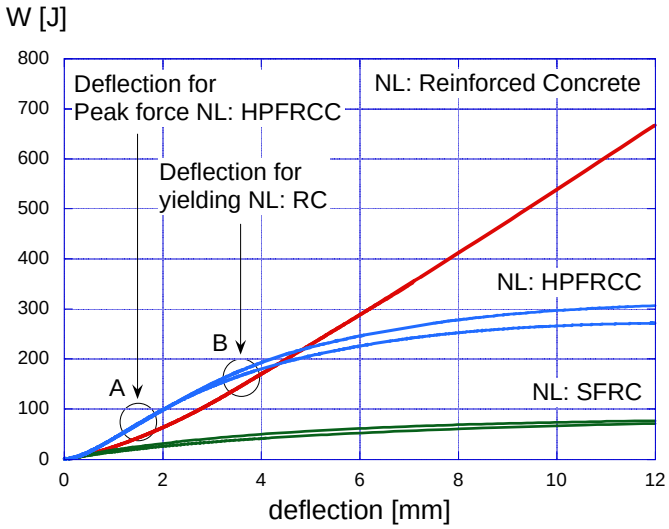


Fig. 6. Experimental tests on the hybrid beams, work-deflection response as a function of the material used for the new layer (NL).

The total energy dissipated by the beams reinforced with HPFRCC is around 300 Joules for a cross section of 220 x 70 mm of the new layer. Neglecting the contribution of the plain old concrete, this means a "specific structural fracture energy" of 300/0.22x0.07 = 19'480 J/m$^2$ that is comparable to the specific fracture energy measured in direct tension. The same energy for SFRC reinforced beams is much smaller, and equal to 5195 J/m$^2$. Compared with the respective amounts of fibers in the two mixes, one gets "relative" specific fracture energies in J.m/kg of 69.3 for SFRC reinforced beams and 118 for the HPFRCC (almost double). This demonstrates that the HPFRCC makes a better use of the energy dissipation potential of the steel fibers, most probably owing to the good bonding provided by the HPFRCC matrix.
Finally, the observed behavior demonstrates that, within a range given by the fibrous reinforcement, the HPFRCC is comparable to usual RC in terms of energy dissipation, not only at a material level, but also at a structural level.

## 3. Numerical modeling of structural response

### 3.1 Discrete crack model - inverse analysis

In a first step, a discrete crack model (ICM – Interface Crack Model) implemented in the program MERLIN [5] was used to identify two multilinear tensile laws by fitting of the experimental results obtained on the hybrid beams reinforced with ACM, [6]. One law had a pure softening behavior (SIM 1), the other had a hardening–softening behavior (SIM 2). The best fit with experimental data, especially in the pre-peak domain, was obtained with a hardening-softening law (SIM 2),
Fig. 7.

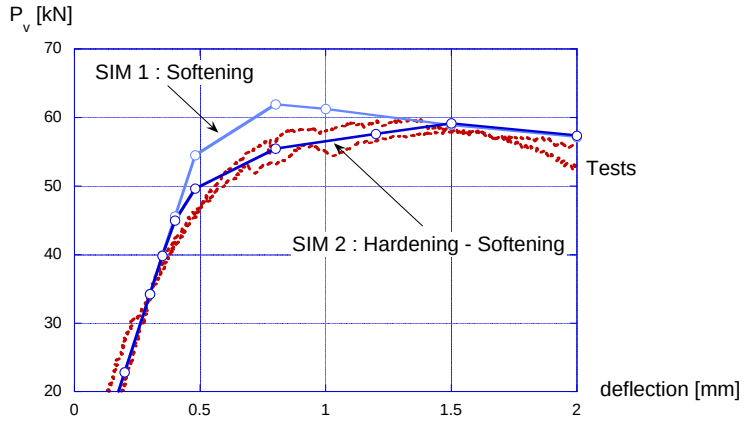


Fig. 7. Comparison of the predictions of a discrete crack model with two tensile laws, with the experimental curves for hybrid beams with HPFRCC.

In a second step, these laws were confirmed by uniaxial tensile tests performed on notched plates with a section of 160 x 50 mm$^2$ extracted from the bottom face of the hybrid beams reinforced with ACM, in the non-loaded zones of the remaining two halves of the beams, after the flexural test was completed, and tested according to the procedure described in § 2.2.
Fig. 8 demonstrates the very good correspondence between the tensile laws determined by inverse analysis and the experimental tensile tests, with full circles indicating the envelope of the experimental tests and empty circles the tensile laws obtained from the inverse analysis.

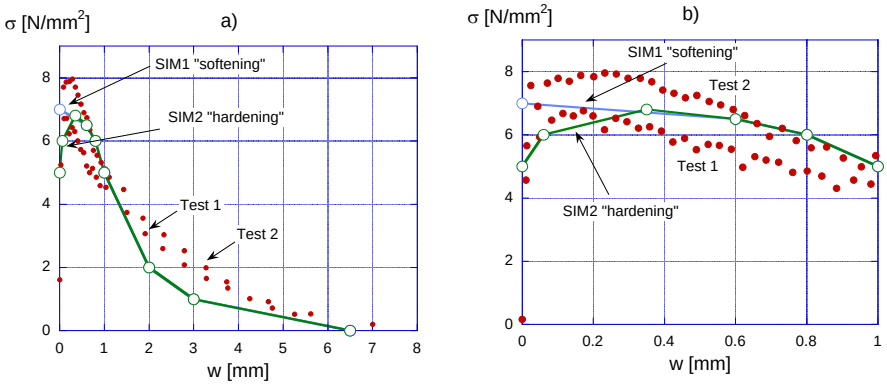


Fig. 8. Tensile laws considered in the simulations and comparison with the experimental tensile tests, a) general, b) detail.

### 3.2 Smeared crack model

In most cases, the discrete crack model imposes to predetermine the position and trajectory of the fracture zone. Moreover, the fracture zone is concentrated on a plane, which is not the case with a smeared crack model applied on the full length of the beam. However, compared to discrete crack models, smeared crack models require the definition of a supplementary parameter: the characteristic length for the normalization of the sigma-w tensile law. In order to check the applicability of such a model, and its robustness, various simulations were performed with the program Heat/MLS [7].

The tensile laws previously determined (SIM 1 and SIM 2) were used with two different options for the definition of the characteristic length: case I) calculated by the program, on the basis of the square root of the determinant of the Jacobian of the finite element considered, or case II) constant numerical value imposed by the user. In both cases, the simulations were performed with a constant mesh, finer in mid span for case I) and with a constant mesh size over the full span for case II).

- In case I), the smeared crack model was imposed on a band centered on mid-span of the hybrid beam, and elsewhere, the materials were supposed to behave linear-elastic. The variable parameter was the width $l_{smeared}$ of the band over which the smeared crack model was imposed.
- In case II), the smeared crack model was imposed on the full beam length and the free parameter was the value of the characteristic length $l_{ch}$,

### 3.3 Smeared crack model – case I: effect of discretization

Fig. 9 and Fig. 10 reveal a strong dependency of the response of the numerical model depending on the width of the zone over which the smeared crack model is imposed. This dependency is largely increased in the case of a hardening-softening law, Fig. 10.

As expected, if the width of the smeared crack diminishes, the response tends towards that obtained for the same tensile law, with a discrete crack model.

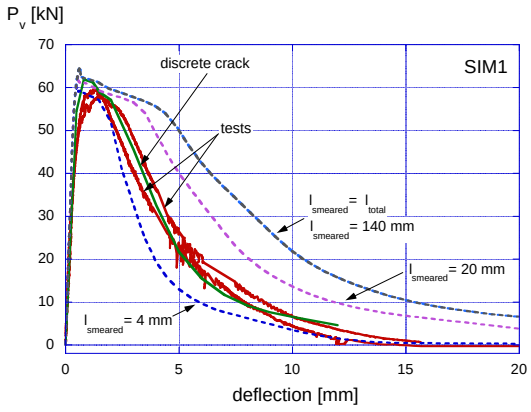


Fig. 9. Comparison between test results and numerical simulations for the tensile law SIM 1 (pure softening), effect of the width over which the smeared crack model is imposed.

On the contrary, with a hardening-softening tensile law, when the smeared crack model is imposed over the full beam length, with a characteristic length determined on the basis of the finite elements geometry, Fig. 10, the response predicted by the program appears to be almost plastic, fully in disagreement with the experimental observations.

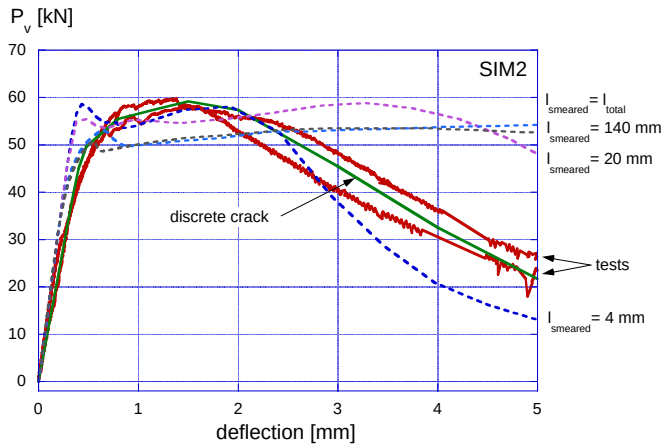


Fig. 10. Comparison between test results and numerical simulations for the tensile law SIM 2 (hardening-softening), effect of the width over which the smeared crack model is imposed.

### 3.4 Smeared crack model – case II: effect of the characteristic length $l_{ch}$

Fig. 11 demonstrates the influence of a constant characteristic length imposed in the smeared crack model, on the full beam length. A value of $l_{ch}$ of 40 to 50 mm appears to provide the best fit with the experimental data. This value can be interpreted either in correspondence with the material parameters (3 to 4 times the fiber length of 13 mm) or with the structural dimensions of the hybrid beam (around 2/3 of the thickness of the new layer in ACM).

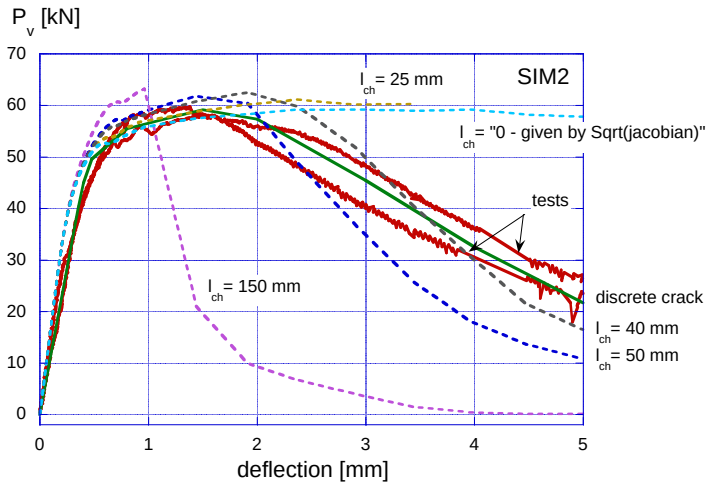


Fig. 11. Comparison between test results and numerical simulations for the tensile law SIM 2 (hardening-softening), effect of the characteristic length $l_{ch}$.

### 3.5 Smeared crack model - distribution of damage

Fig. 12 illustrates for the hybrid beams, the effect of the characteristic length on the extent of the damage at the end of the tests, for a smeared crack model imposed on the full beam length, with a hardening-softening law (SIM 2).

The damage $D_i$ at increment i is defined incrementally as $(1-d_i)$ where $d_i$ is the coefficient by which the modulus of elasticity must be multiplied to follow the stress-strain tensile law in interval i ("secant approach").

In the case of a characteristic length of 150 mm as well as of a characteristic length given by the geometry of the finite elements ($l_{ch}$ = "0"), the extent of the damaged zone is much higher than in the case of a characteristic length of 50 mm. This increased energy dissipation is closely linked to the "quasi-plastic "responses observed in the simulations of the structural response of the beams, Fig. 9, Fig. 10,
Fig. 11.

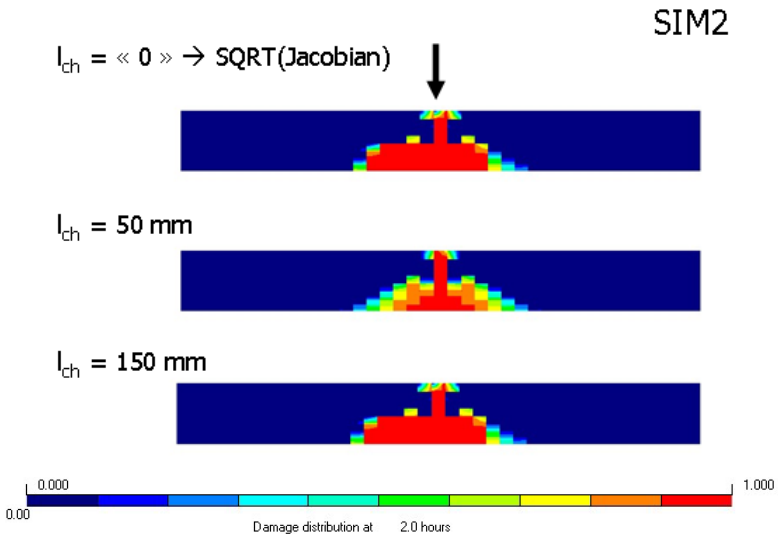


Fig. 12. Effect of $l_{ch}$ on the distribution of damage at the end of the test, hardening-softening tensile law (SIM 2), smeared crack model imposed on the full beam length.

## 4. Conclusions

- The structural response of hybrid beams made of ordinary concrete and HPFRCC is comparable to that of hybrid beams with ordinary concrete and reinforced concrete, in terms of maximum carrying capacity and energy dissipation. It is better in terms of stiffness and cracking behavior at service state.
- The tensile behavior of HPFRCC has been investigated using a uniaxial tensile set-up developed for high tensile strengths.
- The tensile behavior of an HPFRCC was determined by inverse analysis of hybrid beam tests and confirmed by the results of a uniaxial tensile test.
- Most realistic modeling of the structural response of the hybrid beams around the peak was obtained by using a hardening and softening tensile law for the HPFRCC of the new layer.
- Discrete and smeared crack models predict accurately the observed structural response around the peak. Post-peak, along descending branch, discrete crack model performs well. Post-peak, along descending branch, predictions of smeared crack model are strongly influenced by the discretization and the choice of $l_{ch}$ for the HPFRCC in the new layer.
- For smeared crack models, the best results were obtained with an imposed constant characteristic length $l_{ch}$= 40 to 50 mm for the HPFRCC in the new layer, i.e. 4 times the fiber length or 2/3 of the thickness of the new layer $h_{new}$. This trend has to be confirmed on other types of structural elements.

## 5. References

1. Orange G., Acker P., Vernet C., 'A new generation of UHP concrete: Ductal® – damage resistance and micromechanical analysis', in Proceedings HPFRCC3, edited by H.W. Reinhardt and A.E. Naaman, RILEM publications, Proceedings Pro 6, (1999), 101-111.
2. Helbling A., Brühwiler E., 'Eine neue Halterung für Zugversuche mit Beton-Probekörper', *Material und Technik*, No. 4, EMPA Dübendorf, Switzerland, (1987), 103-107.
3. Habel K., Gysler R., Denarié E., Brühwiler E., 'A uniaxial tensile test for Advanced Cementitious Materials', submitted for publication in *Materials and Structures*, (2002).
4. Denarié E, Brühwiler E., 'Comportement d'Eléments de Structure Hybrides formés de Béton Traditionnel et de Matériaux Cimentaires Avancés', Regroupement Francophone pour la Recherche et la Formation sur le Béton $(RF)^2B$, Journées Scientifiques du 30-31 Août 2001, Université Laval – Québec (2001).
5. Reich R., Cervenka J., Saouma V.E., 'MERLIN, A Three-Dimensional Finite Element Program Based on a Mixed-Iterative Solution Strategy for Problems in Elasticity, Plasticity, and Linear and Nonlinear Fracture Mechanics', *EPRI Report*, Palo Alto, (1997).
6. Denarié E., (2000), 'Simulation Numérique du comportement structural d'éléments hybrides formés d'anciens bétons et de Bétons de Fibres à Ultra Hautes Performances', *internal report MCS-EPFL*, (2000).
7. P.E. Roelfstra, A.M. Salet, J.E.Kuiks, 'Defining and application of stress-analysis-based temperature difference limits to prevent early-age cracking in concrete structures'. Proceedings n°25 of the International RILEM Symposium: Thermal cracking in concrete at early age, Munich, (1994), 273-280.

## 6. Acknowledgement

The authors gratefully acknowledge Lafarge for donating the raw materials of DUCTAL®, and Bekaert for donating the Dramix fibers.